IEICE TRANSACTIONS

on Fundamentals of Electronics, Communications and Computer Sciences

DOI:10.1587/transfun.2024EAP1109

Publicized:2024/11/05

This advance publication article will be replaced by the finalized version after proofreading.

A PUBLICATION OF THE ENGINEERING SCIENCES SOCIETY

The Institute of Electronics, Information and Communication Engineers

Kikai-Shinko-Kaikan Bldg., 5-8, Shibakoen 3 chome, Minato-ku, TOKYO, 105-0011 JAPAN

PAPER

Detecting Defect Copper Parts Based on Machine Vision

Zhenhai TAN[*†a)], **Yun YANG**[††], **Xiaoman WANG**[†], ***and*** **Fayez ALQAHTANI**[†††], ***Nonmembers***

SUMMARY The quality detection of copper alloys plays a crucial role in enhancing the factory's economic and production efficiency, particularly in addressing surface defects and ensuring component size and specification accuracy. This paper proposes a deep learning-based quality detection method for detecting the defect on the surfaces of copper alloy components, encompassing both surface defect detection and external dimensional quality assessment. For defect detection, the method achieves an accuracy of 94% with an average detection time of 29ms. In dimensional quality detection, the accuracy reaches 96%, with an average detection time of 3 seconds. Validation confirms that this deep learning-based method significantly improves the factory's detection efficiency.
key words: *Copper alloy components, Quality detection, Deep learning*

1. Introduction

With the continuous development of computer software and hardware, computer technology has been rapidly advancing, computer technology is also developing rapidly [1], [2], Target detection algorithms have also seen significant progress, including Fast-RCNN [3], Faster-RCNN [4], and You Only Look Once version 4 (YOLOv4) [5], which have all demonstrated good results after training. Consequently, there have been gradual improvements in surface defect detection and external dimension quality detection. However, in most factories, quality detection still relies on traditional manual visual methods. These methods suffer from inefficiencies, high costs, high error rates, subjectivity, and susceptibility to individual inspectors' influence.

The objective of this research is to develop a system for detecting defects on the surfaces of copper components using machine vision, addressing both surface defect detection and precision in external dimension measurement. At present, industrial defect detection largely relies on manual operations. This approach is costly, and the results are influenced by human factors. In actual production, workers may experience fatigue and other negative factors, leading to low efficiency and reduced stability in defect detection outcomes. For surface defects, deep learning methods can be utilized to automatically extract defect features, reducing labor costs and enhancing detection accuracy and real-time performance. For small-scale defects, specific improvements to detection algorithms are necessary, such as refining the backbone network to reduce computational resource requirements, optimizing feature fusion modules, and introducing attention mechanisms to enhance the extraction of small-scale defect features. For external dimension specification detection, this study accelerates the process by replacing traditional measurement data methods with deep learning techniques to assess dimensional conformity. Following an initial detection, a template is generated to enable automated detection in future assessments. In summary, our contributions are as follows:

- A dataset of surface defects in copper alloy components is created, and to address the issue of limited initial data, the dataset is augmented using geometric transformations.
- We propose a method based on YOLO7 for detecting possible scratches on the surface of copper components. The model is streamlined for low-computing power application scenarios, and the feature fusion module of YOLOv7 is improved, reducing the number of optimized network parameters and computational costs, making it more suitable for deployment in low-computing power environments.
- • We conduct experiments to compare the features of the processed point cloud model with a reference model and evaluate the external dimensional specifications to achieve accurate dimensional quality inspection.

The rest of this article is structured as follows. Section 2 describes the work in this area. Section 3 describes the proposed method for quality detection of copper components. Experimental results and conclusions are presented in sections 4 and 5, respectively.

2. Related work

Traditional machine vision surface defect detection methods often include the following steps: collecting image data through industrial cameras or other data acquisition equipment; preprocessing of the acquired image data; Feature extraction was performed on preprocessed images; Finally, the target classification and recognition are carried out based on the extracted feature pairs. Graph feature extraction is the most important component step in machine vision. Current target classification and recognition algorithms generally in-

[†]The author is with the School of Public Policy and Administration, Nanchang University, Nanchang 330031, China.
[††]The author is with the School of Civil Engineering and Architecture, Nanchang Hangkong University, Nanchang 330063, China.
[†††]The author is with King Saud University, Riyadh 12372, Saudi Arabia.
a) E-mail: 13036215365@163.com

clude decision trees [6], SVM (support vector machines) [7], and logistic regression [8]. A great deal of research progress has been made in surface defect detection based on traditional machine vision methods [9]- [13]. While traditional machine learning techniques are gradually being integrated with surface defect detection, machine learning requires manual feature extraction. The process is cumbersome, costly, and environmentally friendly. With the development of deep learning [14], [15], some scholars have also proposed some efficient network structures based on convolutional neural networks, such as ResNet [16], AlexNet [17], DenseNet [18], SENet [19], VGGNet [20], etc. On the basis of these efficient networks,a large number of algorithms have been proposed and applied to various surface defect detection [21]- [29].The deep learning network can effectively memorize the surface defect features of copper alloy parts by learning the defect features by itself, and show a more accurate ability to identify the defect features.Traditionally,the quality detection of external dimensions is to determine whether the component size is qualified by measuring the dimensional data. At present, the dimensional measurement of industrial parts is mainly carried out manually. Although the manual operation is simple, its error is large and the subjectivity is strong. With the rapid development of deep learning in various fields [30], [31], machine vision technology has been widely used in the industrial field for accurate measurement of part dimensions [32]- [39].

3. Proposed method

Firstly, the YOLOv7 model is introduced to optimize the backbone network using various lightweight architectures. Based on the specific characteristics of the defects being detected, the feature fusion module is enhanced. Additionally, incorporating attention mechanisms improves the efficiency of feature extraction. For external dimension quality detection, we implemented point cloud classification using PointNet. The input points are first passed through a spatial transformation network, followed by a multi-layer perceptron and a feature transformation process. Afterward, the point cloud features are extracted and integrated through maximum pooling, and finally, classification results are obtained via a multi-layer perceptron. This approach eliminates the need for direct measurements, allowing the system to assess dimensions based on classification.

3.1 Surface defect detection module

Due to the large network of YOLOv7, the training requires a large amount of computing resources. In the later stage of deployment, the network may not be able to adapt well to the production environment, so we improve the network backbone structure to reduce the weight. The improved YOLOv7 network is still divided into backbone network, feature fusion network, and detection network, but its internal network structure has been optimized. We chose to lighten the backbone network based on MobileNetV3 [40]; Integrating the

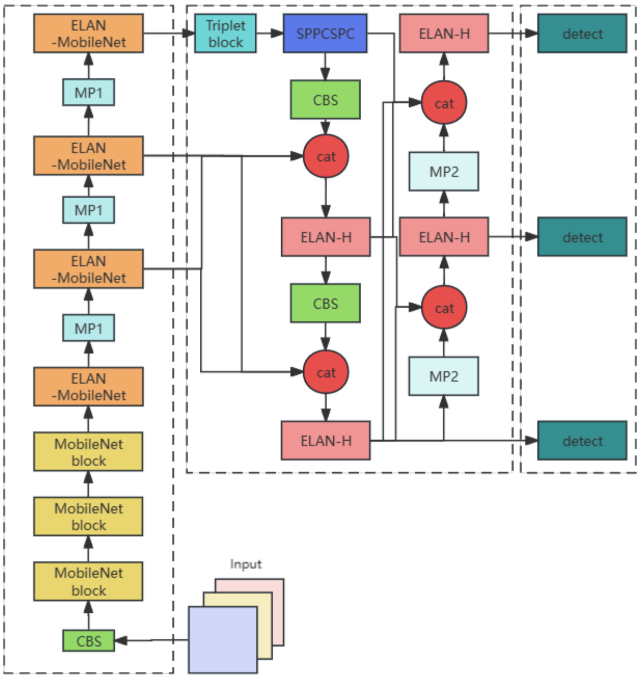

Fig. 1 Surface defect detection framework.

Triplet attention mechanism [41] and using its three-branch structure, the interaction between channels and spatial features is effectively integrated, and the extraction of features is strengthened. In addition, the feature fusion module is optimized, and the adaptability of the network to multi-size defect features is strengthened by introducing progressive features, and the robustness of the network is enhanced. The improved network structure is shown in Fig. 1. The inputs are the samples from NEU-DET dataset.

MobileNet decomposes the convolution operation into deep convolution and point convolution to reduce network parameters and reduce the amount of computation. The standard convolutional kernel in the original network is decomposed into a single-channel mode, allowing convolution operations to be performed independently on each channel without altering the depth of the input feature map. This results in an output feature map with the same number of channels as the input. Subsequently, pointwise convolution is applied to adjust the feature map's dimensions, either increasing or reducing them, while preserving sufficient effective information.

In standard convolution, assume that the size is K*K, the number of channels is M, and the number of channels is N. In this case, the total number of parameters of the convolution can be roughly calculated, and the calculation formula is shown in Eq. (1).

$$K \times K \times M \times N \tag{1}$$

The amount of computation is expressed as follows in Eq. (2):

$$K \times K \times M \times N \times W \times H \tag{2}$$

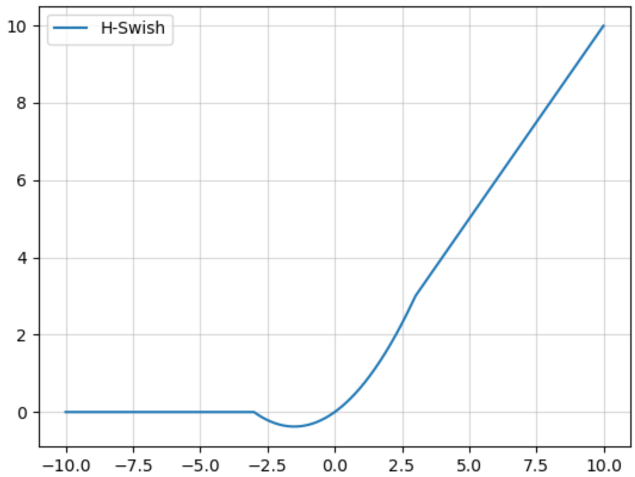

Fig. 2 The plot of H-swish function .

where W and H represent the width and height of the input image, respectively.

For the depth separable convolution, the size of the convolution kernel of the deep convolution part is K*K, the number of channels is M, and the number of channels is 1. The size of the convolution kernel of the point convolution part is 1*1, the number of the kernels is M, and the number of channels is N. The formula for calculating the total number of parameters is shown in Eq. (3):

$$K \times K \times M + 1 \times 1 \times M \times N \tag{3}$$

The amount of computation is expressed as follows in Eq. (4):

$$K \times K \times M \times W \times H + 1 \times 1 \times M \times N \times W \times H \tag{4}$$

Therefore, it can be concluded that after using the depth separable convolution, the parameters and computational quantities of the network are the original. Generally, the size of the convolutional kernel is 3*3, and after optimizing the backbone network of YOLOv7, the number of parameters and computational costs are significantly reduced, which is roughly one-ninth of the original model.

The initial activation function in the vanilla YOLOv7 network is the SiLU function, which has a smoother curve when approaching zero, and because it uses the sigmoid function, the output range of the network is between 0 and 1. The formula for the SiLU activation function is shown in Eq. (5):

$$\mathrm{SiLU}(x) = \frac{1}{(1 + \exp(-x))} \tag{5}$$

However, there is a risk of gradient disappearance in this activation function, and the range of the function is between (0,1), which may lead to the loss of information. However, the H-wish activation function has the characteristics of lower bound, no upper bound, smoothness and non-monotony, which can effectively improve the above shortcomings and suppress the problems of gradient disappearance. However, the H-wish activation function increases the inference delay. Therefore, in this paper, only part of the SiLU activation function is changed to the H-swish activation function. The specific expression of the H-wish activation function is shown in Eq. (6), and the function image is shown in Fig. 2.

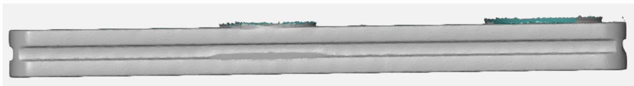

Fig. 3 Initial point cloud visualization.

$$H\text{-}swish(x) = \begin{cases} 0, & x \le -3 \\ x\frac{\mathrm{ReLU6}(x+3)}{6}, & -3 < x \le 3 \\ x, & x > 3 \end{cases} \tag{6}$$

Additionally, we utilize the inverted residual structure. This approach begins by applying a 1x1 convolution to the input, performing an up-dimensional operation that expands the number of channels. This expansion enhances the network's ability to extract features more effectively in higher-dimensional space. Then, a 3x3 deep convolution was used to extract the surface defect image features of the copper alloy components. After that, 1x1 convolution is performed to achieve the goal of dimensionality reduction, and finally, the output is output through a fully connected operation. Through the inversion of the residuals in this paper, the requirements of the backbone network for computing resources are more easily met, and it is conducive to the extraction of features by the model.

3.2 External dimension quality detection module

A visualization image of the initial point cloud data acquired by laser scanning is shown in Fig. 3. From Fig. 3, it can be seen that the initial point cloud data collected has a lot of noise. The noise of point cloud data in the process of point cloud classification will have a huge impact on the training of the network, affect the learning of the point cloud features of the copper element benchmark model, and then affect the classification results.

We use a double-sided filtered point cloud denoising method that takes into account both spatial proximity and feature similarity, which allows it to avoid blurring edges and important features during smoothing. The specific steps are as follows: Calculate the spatial weights. This weight is determined by the Euclidean distance of the point cloud location. The distance between p(i , j),q(k , l) is measured, and the farther the distance, the lower the weight, as shown in Eq. (7). σ_d is the standard deviation of the Gaussian function.

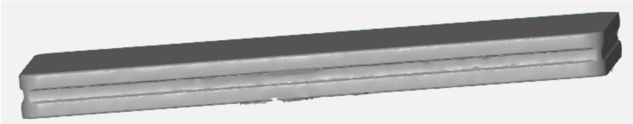

Fig. 4 Point cloud visualization after preprocessing

$$w_d(i,j,k,l) = \exp\left(-\frac{(i-k)^2+(j-l)^2}{2\cdot\sigma_d^2}\right) \tag{7}$$

Calculate range weights. This weight is determined by the difference between the pixel values and measures the degree of similarity between the pixel values of p and q, and the more similar the weight, the greater the weight. The formula for its calculation is shown in Eq. (8). where f(i, j) is the pixel value corresponding to p(i, j), and σ_r is the standard deviation of the Gaussian function.

$$w_r(i,j,k,l) = \exp\left(-\frac{\|f(i,j)-f(k,l)\|^2}{2\cdot\sigma^2}\right) \tag{8}$$

The weight coefficient is calculated using the two weights obtained in the previous step, as shown in Eq. (9).

$$w(i,j,k,l) = w_d(i,j,k,l) * w_r(i,j,k,l) \tag{9}$$

Calculate the output pixels. The output pixels are calculated based on the parameters obtained earlier. The simplified calculation formula is shown in Eq. (10). Repeat the above steps to process all points in the point cloud to obtain the denoised point cloud data.

$$g(i,j) = \frac{\sum_{(k,l)\in S(i,j)} f(k,l)w(i,j,k,l)}{\sum_{(k,l)\in S(i,j)} w(i,j,k,l)} \tag{10}$$

After the noise reduction process of the bilateral filtering algorithm, the point cloud visualization image is shown in Fig. 4. At this point, the noise in the point cloud has been handled, and the edge features in the point cloud are well preserved. The point cloud samples are necessary for defect detection on edge.

For the external dimension quality detection of copper components, we apply a 3D point cloud classification approach based on deep learning. Given the relatively simple shape of the copper components and the need for fast detection, we opted to classify the preprocessed point cloud using PointNet. The network structure for this method is illustrated in Fig. 5. PointNet learns the spatial code corresponding to each point in the input point cloud, and then uses the features of all points to obtain a global point cloud feature. In this process of fusing the point cloud described by n points, the n vectors are turned into a new vector independent of the input order, which can be represented by Eq. (11).

$$f(\{x_1,\ldots,x_n\}) \approx g(h(x_1),\ldots,h(x_n)) \tag{11}$$

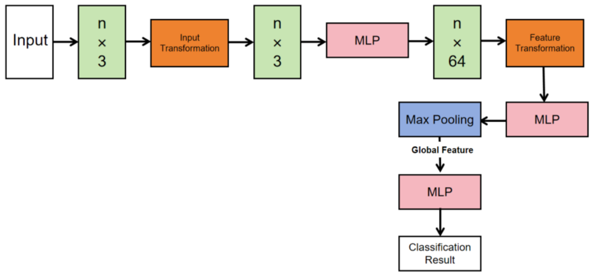

Fig. 5 The structure of attention mechanism in the proposed model.

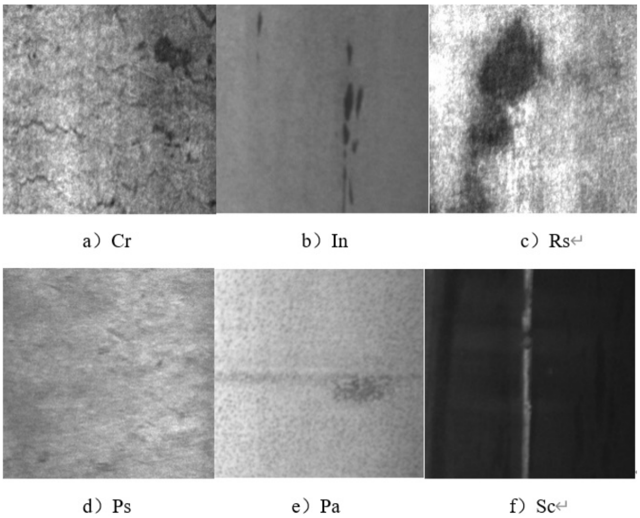

Fig. 6 Defective samples from the NEU-DET dataset.

where f is the target point set, h is the MLP operation, and g is the max pooling operation.

4. Experiments and results

4.1 Dataset

We used the NEU-DET dataset for pre-training to obtain the initial weights, and we enriched the original dataset based on geometric transformations. Six different types of defects are included in the NEU-DET dataset, which are cracks (Cr), inclusions (In), rolled scale (Rs), pitting surfaces (Ps), plaques (Pa), and scratches (Sc). There is a total of 7200 samples in the dataset. All of the images are collected in a factory which produce copper alloy components for cell phones and other electronic devices. Fig. 6 shows a partial map of the surface defects in NEU-DET. Although there are many types of possible defects in industry, our paper primarily focuses on this type of defect, specifically surface scratches. All related experiments and results are centered around this issue.

The area of some defects in this dataset is small, accounting for only 1% or less of the overall image area, and this part of the defects is called small defects, which accounts for 1.17%; Small defects are one of the difficulties in detection. Similarly, the area of medium-sized defects is less than 10% and greater than 1% of the area of the whole image, and this part of the defect accounts for 43.6%; The area of large defects accounts for more than 10% of the whole image, and the defects account for 55.23%.

4.2 Experiment environment settings

All experiments were performed on servers equipped with NVIDIA RTX3090 GPUs using Python and Pytorch libraries. In addition, to optimize the network parameters, the Adam optimizer was used and the learning rate was set to 0.01. In order to enhance the diversity of training samples, we used vertical flipping and horizontal flipping for data augmentation. The size of the input image is 640×640, and the network is trained using a batch size of 16 for a total of 150 epochs.

4.3 Experimental design for surface defect detection

In order to test the enhancement of the detection effect of each improvement, the improved methods of the backbone network based on different lightweight networks were designed and compared experiments were designed with feature fusion layers of different attention mechanisms.

In the comparison experiment, the backbone network of YOLOv7 was replaced with MobileNetV3 and ShuffleNetV2, respectively, and the control experiment was carried out with the original network. The results of the comparative experiments are shown in Table 1, and it can be found that the lightweight improvement of YOLOv7 based on MobileNetV3 and ShuffleNetV2 is effective, and the size of the models trained by YOLOv7 optimized based on MobileNetV3 and YOLOv7 optimized based on ShuffleNetV2 is reduced by 231MB and 221.3MB respectively compared with the original YOLOv7 trained models. The amount of computation is reduced, respectively; The number of parameters is reduced. In terms of detection efficiency, although the mAP@0.5 of the improved YOLOv7 detection model is lower than that of the original network, it is reduced by 3.3% and 2.6%, respectively. However, its FPS has increased by 13 frames per second and 9 frames per second, respectively.

Table 1 Comparison Experiments of YOLOv7 with YOLOv7 Based on Different Lightweight Backbone Networks

Model	Model Size/MB	GFLOPs	Params/M	mAP@0.5	FPS
YOLOv7	277.2	104.7	37.2	0.829	30
YOLOv7 -Mobile	46.2	21.8	5.3	0.796	43
YOLOv7 -Shuffle	55.9	26.7	6.2	0.803	39

Although the effectiveness of the improvement based on the two lightweight networks proposed in this paper has been verified, MobileNetV3 is finally selected as the improvement method of YOLOv7 backbone network lightweight after comparing specific application scenarios and performance.

In the YOLOv7 backbone network, the SPPCSPC layer incorporates the Triplet attention mechanism, SE attention mechanism, and CA attention mechanism. Experiments were conducted using the defect dataset mentioned earlier, with the results displayed in Table 2. While the fusion of Triplet, SE, and CA mechanisms led to some improvement in detection accuracy, the added network complexity reduced real-time detection performance. Since the detection model in this study requires high real-time efficiency, after careful consideration, the Triplet attention mechanism was selected to optimize YOLOv7.

Table 2 Comparison Experiments of YOLOv7 and YOLOv7 with Integrated Different Attention Mechanisms

Model	Params/M	GFLOPs	mAP @0.5	FPS
YOLOv7	37.2	104.7	0.829	30
YOLOv7 -Triplet	37.28	105.8	0.877	29
YOLOv7 -SE	37.56	106.5	0.863	27
YOLOv7 -CA	37.36	106.9	0.882	24

Table 3 Ablation Experiments of YOLOv7 with the Addition of Different Modules

Model	AFPN	MobileNet	Triplet	mAP@0.5	FPS
YOLOv7				0.829	30
YOLOv7-Triplet			✓	0.877	29
YOLOv7-mobile		✓		0.796	43
YOLOv7-AFPN	✓			0.864	23
Improved YOLOv7	✓	✓	✓	0.926	39

Ablation experiments were used to verify whether the improvement based on MobileNetv3, Triplet, and AFPN was effective in improving the detection performance. The results of the ablation experiment are shown in Table 3. In the previous paper, the backbone network is lightweighted, the Triplet attention mechanism is integrated, and the feature fusion module is modified. In Table 3, if modules introduced by previous improvements are added, they are marked with "✓"; If this module is not introduced, it is marked with a blank grid.

As can be seen in the table, despite the MobileNetV3-based backbone lightweight improvements, the improved detection network accuracy is reduced compared to the original network. However, the size of the trained model is significantly reduced, the requirements for computing resources are also reduced, and the real-time performance of network detection is greatly improved compared with other single improvements. Moreover, after the fusion of Triplet and the improvement of the feature fusion module, the detection accuracy is greatly improved compared with the original network.

4.4 External dimension quality detection experiment

In this subsection, a comparative experiment is designed with the manual detection method and laser measurement method of the processing plant proposed in this section. In this experiment, two experiments with a measurement error threshold of 0.05mm and a measurement error threshold of 0.01mm were set up respectively, and each experiment consisted of three sets of experiments. In order to facilitate statistics, 50 standard-size copper alloy components are selected for detection, and if all 50 standard-size copper alloy components are accurately detected, the detection accuracy is 100%. The results of the comparative experiment with an error threshold of 0.05 mm are shown in Table 4, and the results of the comparative experiment with an error threshold of 0.01 mm are shown in Table 5.

Here, manual denotes visual inspection which is performed by human. Visual inspection is a straightforward and cost-effective method but is limited to surface defects and relies heavily on the inspector's skill and experience. The technician inspects the surface of the material or component using the naked eye or aided tools such as magnifying glasses, borescopes, or mirrors, to identify defects like cracks, scratches, dents, or other surface irregularities. Visual inspection is commonly used for quick assessments of surface quality, especially for large components or simpler structures. It is often the first step in defect detection and may be followed by more detailed testing if necessary.

The experiment evaluates the detection accuracy and the average detection time, wherein the manual detection accuracy is compared with the reference element size by comparing the manual measurement size result, and then the detection accuracy is calculated; In this method, the judgment result is directly output, and the detection accuracy is output after the detection is completed. The average detection time is averaged after the detection of 50 standard-size copper alloy components, and then rounded and output.

As can be seen from Table 4 and Table 5, the method in this paper can have good detection accuracy and real-time performance when the measurement error threshold is 0.05mm and the measurement error threshold is 0.01mm. In particular, there is a significant improvement when compares with manual. The adoption of such technology can significantly promote the upgrade of existing techniques and enhance industrial efficiency.

Table 4 Comparison of Detection Specifications with an Error Threshold of 0.05mm

Experiment Group	Detection Method	Detection Accuracy	Average Detection Time/s
1	Proposed	98%	3
	Manual	84%	57
	Laser	98%	8
2	Proposed	96%	3
	Manual	80%	53
	Laser	96%	8
3	Proposed	98%	3
	Manual	72%	60
	Laser	96%	8

Table 5 Comparison of Detection Specifications with an Error Threshold of 0.05mm

Experiment Group	Detection Method	Detection Accuracy	Average Detection Time/s
1	Proposed	94%	3
	Manual	54%	56
	Laser	96%	8
2	Proposed	94%	3
	Manual	62%	63
	Laser	96%	8
3	Proposed	96%	3
	Manual	68%	67
	Laser	98%	8

4.5 Visualization of quality detection results

Through the comparative experiments described in the previous section, it can be concluded that the improved YOLOv7 network has higher detection accuracy and faster detection

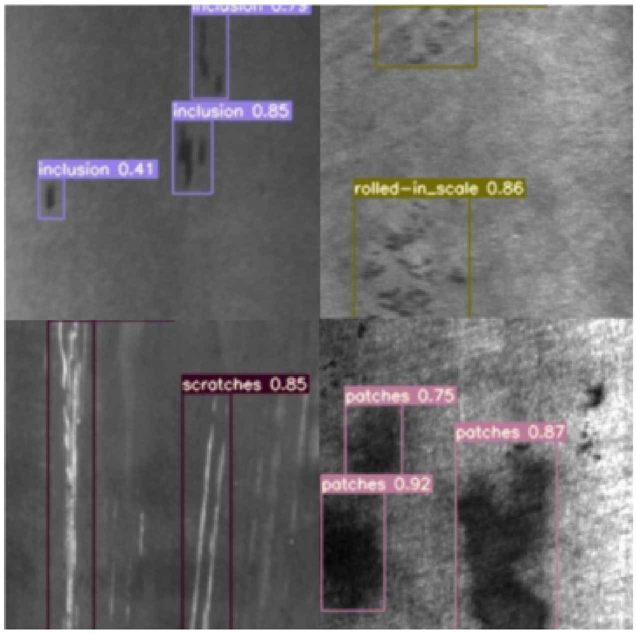

Fig. 8 Improved YOLOv7 quality inspection effect

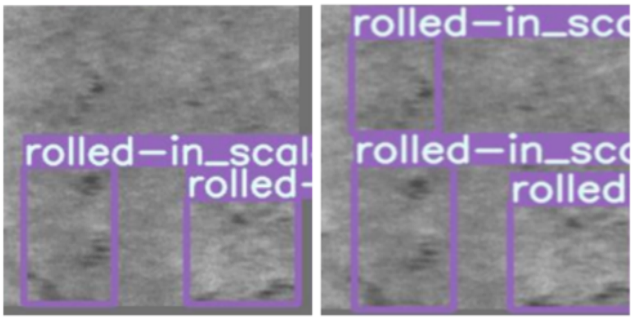

Fig. 7 Comparison of defect detection effect between the original network and the improved network

speed than the original network. Moreover, the network parameters and computational cost are reduced, and the improved detection model is lighter than the original detection model.

Fig. 7 shows the comparison of the original network with the improved network using rolled-in-scale defect detection as an example. The image on the left shows the test results of the original YOLOv7, and the image on the left shows the test results of the improved YOLOv7. Through comparison, it can be found that the original network cannot predict all the detection targets when performing defect detection, and after the improvement of this paper, the targets that the original network does not successfully predict are successfully selected.

Fig. 8 shows the rendering of our improved YOLOv7 for quality detection, whether it is a surface defect or a scale problem in copper components, and can effectively detect small-scale defects in complex backgrounds, such as: inclusions, rolled into oxide scale; As well as a complete box to pick out scratch defects with large scale variations.

5. Conclusion

This study concentrates on quality detection methods for copper alloys, focusing on two main areas: enhancing defect detection algorithms using deep learning and designing an external dimension measurement algorithm based on deep learning. To accommodate low-computing power environments in factories, we streamlined YOLOv7, optimizing the original feature fusion network through progressive feature integration. Additionally, we incorporated an attention mechanism into YOLOv7 to improve the network's generalization capabilities, enhance the model's ability to learn defect features, and further boost detection accuracy. We also designed a set of deep learning-based external dimensional quality detection methods for copper components, which realized the detection of dimensional quality, greatly improved the speed and stability of external dimensional specification detection, and improved the detection accuracy to 0.01mm. Although this study specifically addresses surface scratches on copper components, we believe that, with the necessary adjustments and arrangements, this method can be applied to surface defect detection in components made from other materials as well. In future research, it is hoped that the quality detection of a variety of workpieces will be realized to further improve the economic efficiency of the factory.

6. Acknowledgments

This work was funded by the Researchers Supporting Project Number (RSP2024R509), King Saud University, Riyadh, Saudi Arabia.

References

[1] X. Zhu, F. Ma, F. Ding, et al. “A Low-Latency Edge Computation Offloading Scheme for Trust Evaluation in Finance-Level Artificial Intelligence of Things,” *IEEE Internet of Things Journal*, 2023.

[2] F. Ding, Z. Shen, G. Zhu, et al. “ExS-GAN: Synthesizing Anti-Forensics Images via Extra Supervised GAN,” *IEEE Transactions on Cybernetics*, vol. 53, no. 11, pp. 7162-7173, 2022.

[3] R. Girshick. “Fast R-CNN,” *Proceedings of the IEEE International Conference on Computer Vision*, 2015, pp. 1440-1448.

[4] S. Ren, K. He, R. Girshick, et al. “Faster R-CNN: Towards Real-Time Object Detection with Region Proposal Networks,” *IEEE Transactions on Pattern Analysis and Machine Intelligence*, vol. 39, no. 6, pp. 1137-1149, 2016.

[5] A. Bochkovskiy, C.-Y. Wang, H.-Y. M. Liao. “YOLOv4: Optimal Speed and Accuracy of Object Detection,” *arXiv preprint arXiv:2004.10934*, 2020.

[6] M. Somvanshi, P. Chavan, S. Tambade, et al. “A Review of Machine Learning Techniques Using Decision Tree and Support Vector Machine,” in *2016 International Conference on Computing Communication Control and Automation (ICCUBEA)*, IEEE, 2016, pp. 1-7.

[7] J. Cervantes, F. Garcia-Lamont, L. Rodríguez-Mazahua, et al. “A Comprehensive Survey on Support Vector Machine Classification: Applications, Challenges and Trends,” *Neurocomputing*, vol. 408, pp. 189-215, 2020.

[8] D. W. Hosmer Jr., S. Lemeshow, and R. X. Sturdivant. “Applied Logistic Regression,” *John Wiley & Sons*, 2013.

[9] B. Tang, J. Y. Kong, X. D. Wang, et al. “Image Enhancement and Segmentation of Low-Contrast Micro Defects on Steel Plate Surfaces,” *Journal of Image and Graphics of China*, vol. 25, no. 1, pp. 81-91, 2020.

[10] W. H. Zhao, S. T. Zhou, J. B. Lv, et al. “A Surface Defect Detection Method for Aluminum Profiles Based on Machine Vision,” *Journal of Zhejiang University of Technology*, vol. 49, no. 1, pp. 76-81, 2021.

[11] Z. Liu and B. Qu. “Machine Vision Based Online Detection of PCB Defect,” *Microprocessors and Microsystems*, vol. 82, p. 103807, 2021.

[12] D. Liao, M. Yin, H. Luo, et al. “Machine Vision System Based on a Coupled Image Segmentation Algorithm for Surface-Defect Detection of a Si_3N_4 Bearing Roller,” *JOSAA*, vol. 39, no. 4, pp. 571-579, 2022.

[13] X. Lin, Z. Xu, and J. Chen. “Surface Defect Detection Method for Tungsten Rods Based on Machine Vision,” *Electronics Technology and Software Engineering*, vol. 2023, no. 2, pp. 193-197, 2023.

[14] B. Fan, S. Hu, F. Ding. “Synthesizing Black-Box Anti-Forensics Deepfakes with High Visual Quality,” in *ICASSP 2024-2024 IEEE International Conference on Acoustics, Speech and Signal Processing (ICASSP)*. IEEE, 2024, pp. 4545-4549.

[15] F. Ding, G. Zhu, Y. Li, et al. “Anti-Forensics for Face Swapping Videos via Adversarial Training,” *IEEE Transactions on Multimedia*, vol. 24, pp. 3429-3441, 2021.

[16] K. He, X. Zhang, S. Ren, et al. “Deep Residual Learning for Image Recognition,” in *Proceedings of the IEEE Conference on Computer Vision and Pattern Recognition*, New York, NY: IEEE, 2016, pp. 770-778.

[17] A. Krizhevsky, I. Sutskever, and G. E. Hinton. “ImageNet Classification with Deep Convolutional Neural Networks,” *Communications of the ACM*, vol. 60, no. 6, pp. 84-90, 2017.

[18] G. Huang, Z. Liu, L. Van Der Maaten, et al. “Densely Connected Convolutional Networks,” in *Proceedings of the IEEE Conference on Computer Vision and Pattern Recognition*, New York, NY: IEEE, 2017, pp. 4700-4708.

[19] J. Hu, L. Shen, and G. Sun. “Squeeze-and-Excitation Networks,” in *Proceedings of the IEEE Conference on Computer Vision and Pattern Recognition*, New York, NY: IEEE, 2018, pp. 7132-7141.

[20] K. Simonyan and A. Zisserman. “Very Deep Convolutional Networks for Large-Scale Image Recognition,” *arXiv preprint arXiv:1409.1556*, 2015. [Online]. Available: `https://arxiv.org/abs/1409.1556` [Accessed: 2 April 2023].

[21] G. He and Y. Liang. “PCB Defect Detection Based on Convolutional Neural Network,” *Journal of Graphics*, vol. 43, no. 1, pp. 21-27, 2022.

[22] Z. Zheng, J. Zhao, and Y. Li. “Research on Detecting Bearing-Cover Defects Based on Improved YOLOv3,” *IEEE Access*, vol. 9, pp. 10304-10315, 2021.

[23] Y. Liu, H. Yu, J. Wang, et al. “Multi-Morphology Micro Defect Detection Algorithm for Steel Surface Based on Deep Learning,” *Journal of Computer Applications*, vol. 42, no. 8, pp. 2601-2608, 2022.

[24] L. Zhu. “Research on Workpiece Surface Defect Detection Technology Based on Deep Learning,” [D]. Southwest University of Science and Technology, 2021.

[25] J. Fang and X. Tan. “Metal Surface Defect Detection Algorithm Based on Attention Cascade Network,” *Journal of Frontiers of Computer Science and Technology*, vol. 15, no. 7, pp. 1245-1254, 2021.

[26] Y. He, K. Song, Q. Meng, et al. “An End-to-End Steel Surface Defect Detection Approach via Fusing Multiple Hierarchical Features,” *IEEE Transactions on Instrumentation and Measurement*, vol. 69, no. 4, pp. 1493-1504, 2019.

[27] K. Yang, C. Fang, L. Duan, et al. “Automatic Detection of Casting Defects Based on Deep Learning Model Fusion,” *Chinese Journal of Scientific Instrument*, vol. 42, no. 11, pp. 150-159, 2021. DOI: 10.19650/j.cnki.cjsi.J2108170.

[28] T. Yuan, J. Yuan, Y. Zhu, et al. “Surface Defect Detection Algorithm for Thrust Ball Bearings Based on Improved YOLOv5,” *Journal of Zhejiang University (Engineering Science)*, vol. 56, no. 12, pp. 2349-2357, 2022.

[29] X. Cheng, J. Yu. “RetinaNet with Difference Channel Attention and Adaptively Spatial Feature Fusion for Steel Surface Defect Detection,” *IEEE Transactions on Instrumentation and Measurement*, vol. 70, pp. 1-11, 2020.

[30] F. Ding, B. Fan, Z. Shen, et al. “Securing Facial Bioinformation by Eliminating Adversarial Perturbations,” *IEEE Transactions on Industrial Informatics*, vol. 19, no. 5, pp. 6682-6691, 2022.

[31] F. Ding, K. Yu, Z. Gu, et al. “Perceptual Enhancement for Autonomous Vehicles: Restoring Visually Degraded Images for Context Prediction via Adversarial Training,” *IEEE Transactions on Intelligent Transportation Systems*, vol. 23, no. 7, pp. 9430-9441, 2021.

[32] B. Yang, Q. Huang, R. Guo, et al. “Rapid Detection Method for Key

Geometric Dimensions of Fuel Components Based on Image Optical Flow Stitching," *Nuclear Science and Engineering*, vol. 42, no. 5, pp. 1040-1047, 2022.

[33] F. Zhao, H. Yuan, J. Wu, et al. "Automotive Pipe Flange Dimension Detection System Based on Machine Vision," *Electronic Measurement Technology*, 2023, 46(2): 154–160. DOI: 10.19651/j.cnki.emt.2210498.

[34] K. Feng. "Research on Dimension Measurement and Typical Surface Defect Detection of Metal Mobile Phone Shell Based on Machine Vision," [D]. South China University of Technology, 2018.

[35] S. Lin, H. Ni, B. Li, et al. "Axial Dimension Detection of Bellows Compensator Based on Machine Vision," *Welded Pipe*, 2023, 46(2): 32–40. DOI: 10.19291/j.cnki.1001-3938.2023.02.006.

[36] L. Han. "Measurement Method of Bearing Inner Diameter Size Based on Machine Vision," *Machinery Manufacturing & Automation*, 2020, 49(2): 229–231.

[37] G. Dai, Z. Luo, W. Jiang, et al. "Detection Method for Key Parameters of Small-Sized External Threads Based on Machine Vision," *Manufacturing Technology & Machine Tool*, 2023(8): 161–165. DOI: 10.19287/j.mtmt.10052402.2023.08.023.

[38] H. Ni, B. Li, G. Sui. "Axial Dimension Detection Method of Bellows Compensator Based on Machine Vision," *Electronic Measurement Technology*, 2023, 46(7): 159–164. DOI: 10.19651/j.cnki.emt.2210516.

[39] X. Su, C. Fang, R. Hong, et al. "Positioning and Measurement System for Axial Parts Based on Machine Vision," *Machinery Design & Manufacture*, 2020(7): 250–254.

[40] A. Howard, M. Sandler, G. Chu, et al. "Searching for MobileNetV3," in *Proceedings of the IEEE/CVF International Conference on Computer Vision*. 2019, pp. 1314–1324.

[41] D. Misra, T. Nalamada, A. U. Arasanipalai, et al. "Rotate to Attend: Convolutional Triplet Attention Module," in *Proceedings of the IEEE/CVF Winter Conference on Applications of Computer Vision*. 2021, pp. 3139–3148.

Yang Yun works at the School of Civil Engineering and Architecture, Nanchang Hangkong University, and graduated from Chongqing University with Master's degree. His research direction is project management and machine learning.

Zhenhai Tan received his Bachelor of Science degree in Mathematics and Applied Mathematics from Guangxi University. Then he continued his studies at Nanchang University, and successively completed the master's program in Library Information and Records Management, and obtained the Master of Management. Currently, he is doing her Ph.D. research in Management Science and Engineering. His research focuses on information behavior, digital literacy, and information management with artificial intelligence. He has a keen interest in how artificial intelligence technologies can be used to improve information access and management processes and is committed to exploring cutting-edge issues in this area. In terms of academic research, he has achieved certain results and published three SCI papers and one EI paper.

Xiaoman Wang Wang Xiaoman, born in 1999, is a master's student at the School of Public Policy and Management, Nanchang University. Her research interest lies in computer vision, machine learning, and intelligent industry.

Fayez Alqahtani is currently a Professor with the Software Engineering Department, College of Computer and Information Sciences, King Saud University (KSU). He was appointed as the Director of the Computer Division at the Deanship of Student Affairs. He is also a member of a number of academic and professional associations, such as the Association for Computing Machinery (ACM), the Australian Computer Society, and the Association for Information Systems. He has conducted research projects in several areas of information and communication technology, such as Web 2.0, information security, enterprise architecture, software process improvement, the Internet of Things, and fog computing. He has participated in several academic events.